American Journal of Biochemistry and Biotechnology

Original Research Paper

Design and Experiment on Rotary Cutting Test Bench for Sweet Potato Vine

[1,2]Guizhi Mu, [1]Zhengduo Liu, [3]Junming Liu, [1,2]Wenxiu Zheng, [1]Xieteng Qi, [1]Xu Wang and [1,2]Zhaoqin Lü

[1]College of Mechanical and Electrical Engineering, Shandong Agricultural University, Tai'an 271018, China
[2]Shandong Provincial Key Laboratory of Horticultural Machineries and Equipment, Tai'an 271018, China
[3]Shandong Tai'an Institute of Metrology, Tai'an 271018, China

Article history
Received: 14-08-2021
Revised: 16-01-2022
Accepted: 20-01-2022

Corresponding Author:
Wenxiu Zheng
College of Mechanical and Electrical Engineering, Shandong Agricultural University, Tai'an 271018, China
E-mail: wenxiu9013@163.com

Abstract: To study the cutting mechanism of sweet potato vine, provide technical support and a theoretical basis for the development of sweet potato vine harvesting machinery and improve the resource utilization rate of sweet potato vine, a cutting test bench for sweet potato vine was designed. The test bench consists of two parts: The mechanical part and the measurement-control part. In this study, the requirements for the mechanical structure design of the test bench are first put forward and then the structure and hardware of the measurement control system are described. Using this platform, the cutting experiment of sweet potato vine was carried out and the effects of cutter roller speed, conveying speed and feeding amount on cutting torque, cutting power, and cutting force were deeply discussed. The test shows that the sweet potato cutting test bench not only realizes the visualization of the test process but also has the characteristics of small measurement error, stable operation, and simple operation. Through experiments, when the cutter roller speed is 1266 $r \cdot min^{-1}$, the conveying speed is 0.54 $m \cdot s^{-1}$ and the feeding amount is 1.0 kg, the sweet potato vine cutter has excellent working performance such as high processing efficiency and low energy consumption. The platform can provide a reliable scientific basis for cutter design and power selection of sweet potato vine harvesting machinery.

Keywords: Sweet Potato Vine, Harvesting Machinery, Cutter, Test Bench, Measurement-Control System

Introduction

Sweet potato is a typical dicotyledonous plant of the Convolvulaceae family that is believed to have originated in tropical America. It is widely grown as a food crop in the world and is considered to be an important economic crop, after wheat, rice, and maize (Bovell-Benjamin, 2007). The main commercial producers of sweet potatoes are China, Indonesia, Vietnam, Japan, India and Tanzania, and Uganda (Gibson, 2013). As well as being a major source of food, animal feed, and industrial raw materials, sweet potatoes have even been employed in clinical therapy in China. Many nutritionists believe that sweet potatoes promote health because of their high vitamin and trace element contents while being low in fat and cholesterol (Luthuli *et al*., 2019; Yuan *et al.*, 2016). China is the world's largest sweet potato producer. The annual planting area of sweet potatoes in china is more than 6 million h m^2, accounting for 4.2% of China's total cultivated land, accounting for about 60% of the world's sweet potato planting area (Lu *et al*., 2015; Chen,2020).

The yield of sweet potato vine is generally more than 30 $t \cdot hm^{-2}$. The vines contain rich nutrients, which is an ideal feed material (Pedrosa *et al*., 2015; Pereira *et al.*, 2021). The mechanized harvesting of sweet potato vine is an important link to realizing the whole process of mechanization of sweet potato production and it is also a bottleneck restricting the development of the sweet potato industry (Kakahy *et al*., 2014; Phesatcha and Wanapat, 2013; Kakahy *et al*., 2014). When studying the sweet potato vine harvesting machinery, the cutting mechanism of sweet potato vine directly affects the harvesting efficiency of sweet potato vine, which is an important factor in developing the harvesting machinery (Smith and Wright, 1994). In recent years, the research on the cutting test of crop stalks has received widespread attention and related research is also increasing day by day. Xue *et al.* (2019) took cassava stalks at harvest time as the research object and carried out a cassava stalk cutting experiment on the self-developed cutting test bench. The single-factor and multi-factor tests on the maximum cutting force and power consumption were carried out through the factors such as blade angle, cutter head inclination angle, cutting angle, cutter head rotation speed, machine forward speed, and so on. Wang *et al*. (2022) designed a proposed cutting type cutting test bed of sunflower stem. the cutting speed, the sliding cutting angle, and the cutting angle of the blade for cutting energy consumption was studied. Du *et al*. (2020) designed a biomimetic cutting blade that combined the shape biomimetic technique with the structure and kinematic parameters of the cutting blade. The cutting performance of a biomimetic cutting blade is analyzed by the finite element modeling and actual cutting performance test. Deng *et al*. (2013) designed a disc-type corn stalk cutting test bed and the corn stalks cutting process was studied with high-speed photography. Liu *et al*. (2015) developed a test-bed for straw crushers, which can collect the speed and torque of the pulverizer in real time and accurately. Zhang *et al*. (2013) designed a measure-control system for the stalk cutting test bench, which realized the acquisition and display of cutting torque, cutting force, cutting speed, feeding speed, and other signals. In addition, some scholars have developed a measurement and control platform for cutting wheat and rice. However, there are few studies on the cutting mechanism test platform for sweet potato vine. Only a few scholars use the universal testing machine to study the mechanical properties of sweet potato vine (Hu *et al*., 2015). To solve the above problems, a testing platform for the cutting mechanism of sweet potato vine was designed and manufactured based on Lab view software. The platform can carry out continuous cutting experiments at high speed. It can synchronously collect information such as the rotating speed, torque, and power of the cutter shaft in the cutting process. It provides a theoretical basis and technical support for the design and improvement of sweet potato vine harvesting machinery.

Overall Structure and Working Principle

The sweet potato vine cutting test bench is mainly composed of a feeding and conveying device, cutting device, and measuring and controlling device, as shown in Fig. 1. It can complete the feeding, cutting, and data acquisition of the sweet potato vine at one time.

At the beginning of the experiment, the sweet potato vines were placed on the conveying device, the computer was turned into the interface of the measurement-control system; the cutting motor was started and the rotation speed of the cutting motor was adjusted to make the rotation speed of the cutter shaft meet the requirements set by the test. Then the stepping motor was started and the rotation speed of the motor was adjusted to make the feeding speed of the sweet potato vine can meet the requirements set by the test. Finally, the data acquisition system was started and the signals of the dynamic torque sensor were acquired in real-time. After the test is completed, the collected test data is saved for later experimental analysis. The cutting principle is shown in Fig. 2.

Cutting Device

The cutting device is the key component of the sweet potato vine cutting test bench and its main function is to complete the cutting of the sweet potato vine. The cutting device consists of a rotary cutter, transmission mechanism, asynchronous motor, and fixed frame, the rotary cutter is shown in Fig. 3. When working, the asynchronous motor is started to drive the cutter to realize the cutting motion, and the speed of the motor is adjusted by the frequency converter to ensure that the cutter reaches the cutting speed required for the test. The parameters of the asynchronous motor are as follows: The model is Y100 L-2, the rated voltage is 220V, the rated power is 2.2 kW, the rated speed is 2830r/min and the mass is 38 kg.

The cutting blades are straight-edged. Three straight-edged blades are installed symmetrically along the circumferential direction of the cutter shaft. The cutting performance is stable and the power consumption is small by using a symmetrical arrangement. The centrifugal force generated on the blade can be balanced correspondingly when the machine works and the stability of the machine is good. At the moment when the cutter begins to cut the vine layer with thickness h, the force on the blade is as shown in Fig. 4 and 5.

The reaction force acting on the cutting edge surface pressure is as follows:

$$R = R_{zg}\sin\beta + R_d\cos\beta \tag{1}$$

where R_{zg} represents the reaction force of the extruded vine layer to the cutter; R_d represents the reaction force of the cutting edge to the pressure of the vine layer.

Friction force of cutting edge surface:

$$T_2 = \mu R = u\left(R_{zg}\sin\beta + R_d\cos\beta\right) \tag{2}$$

where $\mu = tg\varphi$ u represents the friction coefficient.

Vertical projection of the friction:

$$\begin{aligned} T_2' &= \mu R\cos\beta = u\left(R_{zg}\sin\beta + R_d\cos\beta\right)\cos\beta \\ &= \mu\left(R_{zg}\frac{\sin 2\beta}{2} + R_d\cos^2\beta\right) \end{aligned} \tag{3}$$

To achieve cutting, the pressure P of the cutting edge must satisfy the following conditions:

$$P \geq R_c + R_{zg} + T_1 + T_2' \tag{4}$$

where, T_1 represents the friction force of the cut vine layer to the cutting edge; R_c represents the reaction force of the cut vine layer to the blade, which can be expressed by the following formula:

DOI: 10.3844/ajbbsp.2022.129.140

$$R_c = tl\sigma_c$$

where *t* is the thickness of the blade, *l* is the length of the blade, and s is the compressive stress of the material.

To analyze the relationship between R_{zg} and R_d, it is necessary to analyze the effects of unit forces dR_{zg} and dR_d acting on the cutting edge. First, the concept of relative density Ɛ is introduced:

$$\varepsilon = \frac{h_x}{h} \approx \frac{\sigma}{E} \tag{5}$$

where, σ represents extrusion stress of the vine material, N·mm^{-2}; E represents elastic modulus, N·mm^{-2}.

Reznik and Pustygin believe that when many crop stalks are extruded, their stress and strain conform to Hooke's Law, that is, the law of elastic deformation. However, Reznik emphasized that with the increase of the depth of the cutting edge into the stem layer, the pressure surface of the cutter increases, and the increased area can be expressed by the following formula:

$$dF_x = ldh'tg\beta \tag{6}$$

The relationship between ε and σ is not directly proportional, but they have some exponential function relationship. Under given conditions, the equation can only explain the dependence of the force R_{zg}on on the variable ε. Therefore, Reznik suggests assuming that $\sigma = R_{zg}/F$, similar to the simple calculation of tensile and compressive strength, under this assumption, the unit forced R_{zg} acting on the plane with width d_x and length $l = 1$ can be written as:

$$dR_{zg} = \sigma dx = E\varepsilon dx = E\varepsilon dh'tg\beta \tag{7}$$

Substitute ε of Formula (5), we can get:

$$dR_{zg} = E\frac{h_x}{h}dh'tg\beta \, R_{zg} = \frac{E}{h}tg\beta\int_0^{h'} h_x dh' = \frac{E}{2h}h'^2 tg\beta \tag{8}$$

ε_1 indicates the relative displacement of the cut vine, that is, its relative deformation in the horizontal direction and the unit reaction force caused by the lateral pressure of the cutting edge surface is as follows:

$$dR_d = \varepsilon_1 Edh' \tag{9}$$

According to engineering mechanics, the relationship between ε and ε_1 is $\varepsilon_1 = \varepsilon_v$, where v is Poisson's ratio.

Substitute ε of Formula (5), we can get:

$$\varepsilon_1 = v\frac{h_x}{h} R_d = v\frac{E}{h}\int_0^{h'} h_x' dh' = v\frac{E}{2}\cdot\frac{h'^2}{h} \tag{10}$$

Since the Poisson's ratio is very small when extruding fluffy materials, R_d is equal to R_{zg}multiplied by a small coefficient. The resultant force of the blade pressure is:

$$P = t\sigma_c + Eh'^2 tg\beta + \frac{u'E}{2}\cdot\frac{h'^2}{h} + u \left(\frac{Eh'^2}{2h}tg\beta\sin^2\beta + \frac{u'E}{2}\cdot\frac{h'^2}{h}\cos^2\beta\right) \tag{11}$$

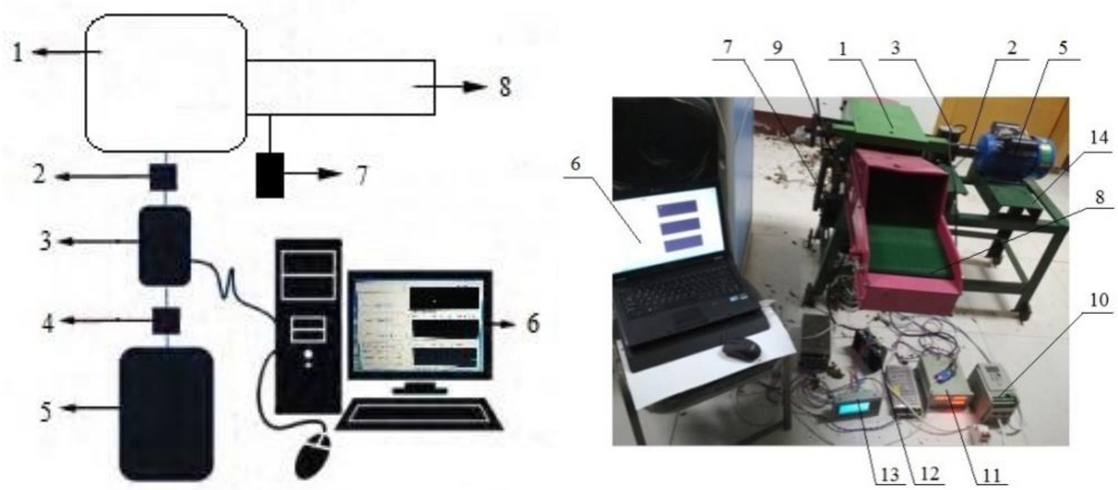

Fig. 1: Schematic diagram and physical diagram of test bench 1. Cutting system2. Coupling 3. Torque sensor 4. Coupling 5. Asynchronous motor 6. Detection program 7. Stepping motor 8. Conveyor belt 9. Feed roller 10. Frequency converter 11. Dynamic torque tester 12. DM860H driver 13. MCU motion controller 14. Fixed frame

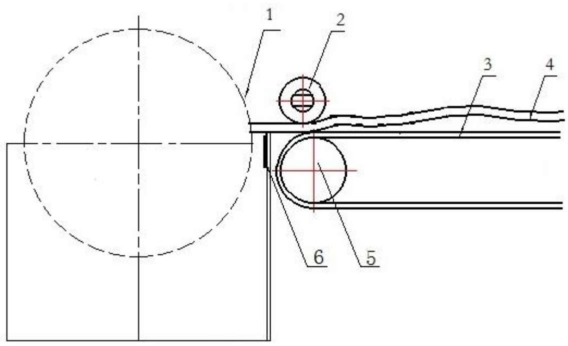

Fig. 2: Cutting principle diagram 1. Cutter 2. Feed roller 3. Conveyor belt 4. Sweet potato vine 5. Conveying driving roller 6. Fixed blade

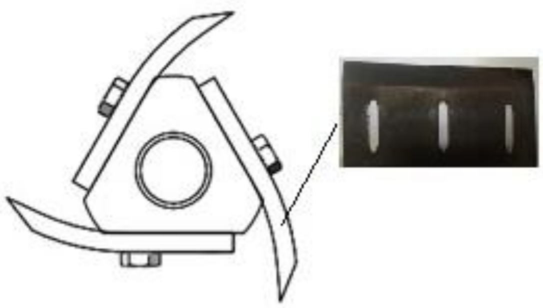

Fig. 3: Schematic diagram of the cutting shaft

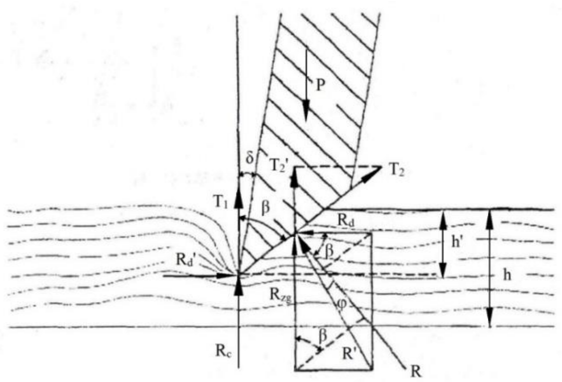

Fig. 4: Force analysis diagram of the moment when the cutter cuts the vine layer

After conversion:

$$P = t\sigma_c + \frac{E}{2}\cdot\frac{h'^2}{h}\left[tg\beta + u\sin^2\beta + u'(u+\cos^2\beta)\right] \quad (12)$$

where u' represents the internal friction coefficient of extruded material.

It can be seen from the above formula that the magnitude of the pressure P acting on the cutting edge is affected by the yield strength of the material σ and the thickness t of the cutting edge. σ can only be determined by the test method, which is related not only to the physical and mechanical properties of the stem material but also to the sharpness of the blade. The other items in the formula are useless resistance. The value of these resistances is proportional to the compression depth h'^2 of the stem layer, inversely proportional to the total thickness h of the stem layer, and has a certain relationship with the elastic modulus E of the stalk, the cut angle β, the friction coefficient μ between the cutter and the material and the internal friction μ' of the material.

Feeding and Conveying Device

The function of the feeding and conveying mechanism is to feed the sweet potato vine to the cutting device at a certain speed. It is mainly composed of a feeding roller, conveyor belt, protective cover shell, etc. The feeding roller has grooves to increase the material gripping ability. The power of the feeding and conveying device is independent and the 86 stepping motor is used to drive the feeding roller and the belt conveying roller to rotate. The working principle of the stepping motor is that when the uniform pulse signal emitted by the MCU motion controller enters the stepper motor driver, it will be converted into a strong current signal required by the stepper motor to drive the stepper motor to run. Whenever the driver receives a pulse, it will give the motor a pulse to rotate the motor at a fixed angle. The stepper motor controller can accurately control the stepper motor to rotate at every angle. The driving of the stepper motor is realized according to the pulse counting, so it has the advantages of fast response and high driving precision. Selecting the DM860H driver to send pulse signals to 86 stepper motors in the test system can realize the functions of short circuit, over-current, and overheat protection and the output current can be continuously adjusted to make the stepping motors rotate more smoothly and continuously. Different feeding speeds can be obtained by adjusting the rotating speed of the stepper motor.

Measurement and Control Device

The hardware of the measurement-control system of the test bench is mainly composed of a torque sensor, dynamic torque measurement-control instrument, and computer. The model of the torque sensor is JN-DN (Bengbu Sensor System Engineering Co., Ltd.), the torque range is 20N·m and the accuracy is 0.002. The model of the dynamic torque measurement-control instrument is MCK-DN (Bengbu Sensor System Engineering Co., Ltd.), the input voltage is 24 VDC and the format of sending and receiving commands is ASCII code. Because the dynamic torque measurement-control instrument can only read in the display window, the real-time data cannot be saved, so through the RS485 interface connected with the data acquisition card of the computer, it can display and record the test data synchronously in the computer and realize the real-time data acquisition.

The control program of the data acquisition system uses LabVIEW software as the development platform to realize the detection of the cutter shaft speed, cutting torque, and cutting power (Xu *et al.*, 2017). The program uses computer serial port technology to realize real-time acquisition, processing, and display of signals such as rotational speed, torque, and power of the cutter shaft. The control program uses a two-layer sequence structure. The first layer of the structure uses a timing cycle and sets every 50 ms as a cycle. When a cycle starts, the program will transmit the acquisition command to the torque sensor, after the torque sensor receives the acquisition command, the real-time voltage and current signals will be encoded into character strings and transmitted back to the second layer of the sequential structure of the program. After receiving the string signal, the program first needs to check the string to ensure the real validity of all data and the accuracy and stability of the system program. Then the string is interpreted to separate the torque signal, the rotation speed signal, and the power signal, and then the signals are transcoded and displayed in the front panel as waveforms and digital characters. Finally, all data is stored in a specified folder as a spreadsheet.

Materials and Methods

Test Materials

The test materials were selected from the sweet potato planting base of Shandong Agricultural University. The sweet potato vines in the harvest period were selected. The variety was Shangshu 19 and the sampling time was October 12, 2021. The water content was 80% and the average length of sweet potato vines was 1.9 m.

Test Methods

To study the significant degree of various factors on the cutting mechanism of sweet potato vines, an orthogonal experiment is needed. Box-Behnken experimental design was adopted in this experiment. The response surface test was carried out with the cutting torque, cutting force, and cutting power consumption as test indexes, taking the cutter roller speed, conveying speed, and feeding amount as test factors. The experimental factors and levels are shown in Table 1.

Cutting torque $\bar{M}$： If the maximum working torque is determined to be M_{ax} in the sampled data, then the formula for calculating the average torque in the cutting area is as follows:

$$\bar{M} = \frac{1}{n}\sum_{i=1}^{n} M_i \tag{13}$$

where $\bar{M}$ represents the average cutting torque; M_i represents the sampling point torque; n represents the number of data collected in the working section.

Cutting power $\bar{P}$: If the maximum working power is determined to be P_{max} in the sampled data, then the formula for calculating the average power is as follows:

$$\bar{P} = \frac{1}{n}\sum_{i=1}^{n} P_i \tag{14}$$

where $\bar{P}$ represents the average cutting power, P_i represents the sampling point power, *and n* represents the number of data collected in the working section.

Cutting force F:

$$F = \bar{M}/R \tag{15}$$

where $\bar{M}$ represents the average cutting torque, *and R* represents the radius of the cutter shaft.

Results and Analysis

Test Results

According to the factor level table and the Box-Behnken test design method, the test scheme and test results are shown in Table 2.

Establishment of Regression Model and Analysis of Variance

The response surface regression model of the cutter roller speed, the conveying speed, and the feeding amount to the cutting torque, cutting power consumption, and cutting force was established by using Design-Expert 8.0 software and the variance analysis was carried out on the regression model. The results are shown in Table 3.

According to the results of variance analysis in Table 3, the model significance P values of the cutting torque, cutting power, and cutting force are all less than 0.01, indicating that the regression model is highly significant. The lack of fit indicates the degree of fitting between the model and the test. Generally, the lack of fit P is greater than 0.05 and the lack of fit in the table is greater than 0.05, indicating that there are no mismatch factors and indicating that the regression equation has a high degree of the fitting. The regression model can be used instead of the real point of the test to analyze the test results. The size of the F value indicates the influence degree of each factor on the cutting torque, cutting power, and cutting force. The larger the F value, the higher the influence degree. The order of significance of each factor on the

DOI: 10.3844/ajbbsp.2022.129.140

cutting torque is the cutter roller speed, the feeding amount, and the conveying speed; the order of significance of the cutting power is the feeding amount, the conveying speed, and the cutter roller speed; the order of significance of the cutting force is the cutter roller speed, the feeding amount and the conveying speed. The test uses the correction coefficient R^2 to indicate the degree of fitting of the selected model, that is, the correlation between the predicted value and the actual value. Generally, R^2 is required to be ≥0.8. Through variance analysis, the determination coefficients R^2 of the cutting torque, cutting power, and cutting force were 0.9609, 0.9599, and 0.9607, respectively, indicating that only 3.91, 4.01 and 3.93% of the variation of the model could not be solved by the model (1-0.9609 = 0.0391, 1-0.9599 = 0.0401,1-0.9607 = 0.0393), indicating that the model has a good fitting degree and can be used for experimental prediction.

For the cutting torque Y_1, factors *A*, *C*, *and* A^2 were highly significant ($P<0.01$), *B*, *and AC* were significant ($P<0.05$); for cutting power Y_2, factors *B*, *C*, and A^2 were highly significant ($P<0.01$), *A*, *AC*, *BC* was significant($P<0.05$); for the cutting force Y_3, factors *A*, *C*, A^2 were highly significant ($P<0.01$), *B*, *AC* were significant ($P<0.05$).

The results of Table 3 were carried out with multiple regression analysis by using Design-Expert8.0 software. A quadratic polynomial response surface regression model of the cutting torque, cutting power and cutting force and the test factors (cutter roller speed, conveying speed, and feeding amount) was established, as shown in Eq. (16) to (18):

$$\begin{aligned} Y_1 &= 1.23 - 0.24A + 0.07B + 0.11C - 0.013AB + 0.075AC \\ &-0.0075BC + 0.11A^2 + 0.018B^2 - 0.034C^2 \end{aligned} \tag{16}$$

$$\begin{aligned} Y_2 &= 155.6 + 6.38A + 12.25B + 13.38C + 1.75AB \\ &+6.5AC + 6.75BC + 16.45A^2 - 1.3B^2 + 1.45C^2 \end{aligned} \tag{17}$$

$$\begin{aligned} Y_3 &= 10.28 - 2.03A + 0.59B + 0.89C - 0.11AB \\ &+0.63AC - 0.06BC + 0.92A^2 - 0.15B^2 - 0.28C^2 \end{aligned} \tag{18}$$

Based on ensuring the model $P<0.01$ and the lack-of-fitting term $P>0.05$, the non-significant regression terms of the model were eliminated and the models Y_1, Y_2, and Y_3 were optimized, as shown in Eq. (19) to (21):

$$Y_1 = 1.23 - 0.24A + 0.07B + 0.11C + 0.075AC + 0.11A^2 \tag{19}$$

$$\begin{aligned} Y_2 &= 155.6 + 6.38A + 12.25B + 13.38C \\ &+6.5AC + 6.75BC + 16.45A^2 \end{aligned} \tag{20}$$

$$Y_3 = 10.28 - 2.03A + 0.59B + 0.89C + 0.63AC0.92A^2 \tag{21}$$

Analysis of Two-Factor Interaction Effect

According to the analysis results of the above regression equation, the response surface methodology was used to investigate the effects of the interaction of cutter roller speed *A*, conveying speed *B*, and feeding amount *C* on the cutting torque Y_1, cutting power Y_2, and cutting force Y_3, as shown in Fig. 6.

The effect of interaction factors on the cutting torque Y_1 is shown in Fig. 6(a)-6(c). Figure 6(a) to 6(c) are response surface diagrams of the interaction between the cutter roller speed *A* and the conveying speed *B*, the cutter roller speed *A* and the feeding amount *C* and the conveying speed *B* and the feeding amount *C* on the cutting torque Y1, respectively. It can be seen from Fig. 6(a)-6(c) that the cutting torque decreases with the increase of the cutter roller speed and increases with the increase of the conveying speed and feeding amount. When the cutter roller speed increases, the cutting resistance decreases, so the cutting torque decreases; when the conveying speed and the feeding amount increase, the cutting resistance increases, so the cutting torque increases.

The effect of interaction factors on the cutting power Y_2 is shown in Fig. 6(d)-6(f). Fig. 6(d) to 6(f) are response surface diagrams of the interaction between the cutter roller speed *A* and the conveying speed *B*, the cutter roller speed *A* and the feeding amount *C* and the conveying speed *B* and the feeding amount *C* on the cutting power Y_2, respectively. It can be seen from Fig. 6(d)-6(f) that the cutting power decreases first and then increases with the increase of the cutter roller speed and increases with the increase of the conveying speed and feeding amount. When the cutter roller speed increases, the cutting resistance decreases, on the other hand, the exhaust resistance caused by the rotating hob increases. As the rotational speed of the cutter shaft increases, the reduction of the cutting resistance at the beginning exceeds the increase of the exhaust resistance, so the cutting power decreases. With the further increase of the rotational speed of the cutter shaft, the exhaust resistance and the impact resistance of the sweet potato vine after cutting increase together more than the reduction of the cutting resistance, so the cutting power increases again. As the conveying speed and feeding amount increase, the cutting resistance increases, so the power consumption increases.

The effect of interaction factors on the cutting force Y_3 is shown in Fig. 6(g)-6(i). Fig. 6(g) to 6(i) are response surface diagrams of the interaction between the cutter roller speed *A* and the conveying speed *B*, the cutter roller speed *A* and the feeding amount *C* and the conveying speed *B* and the feeding amount *C* on the cutting force Y_3, respectively. It can be seen from Fig. 6(g)-6(i) that the cutting force decreases with the increase of the cutter roller speed and increases with the increase of the conveying speed and feeding amount. The overall influence trend of various factors on cutting force is that the higher the cutter roller speed, the slower the conveying speed, and the smaller the feeding amount, the smaller the cutting force will be.

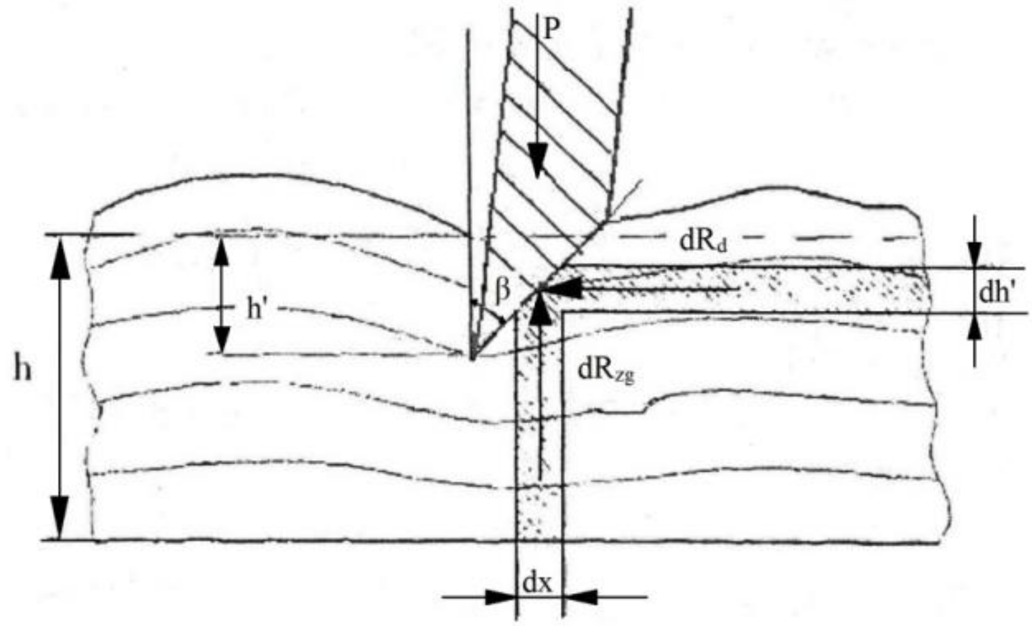

Fig. 5: The pressure unit surface of the cutting edge

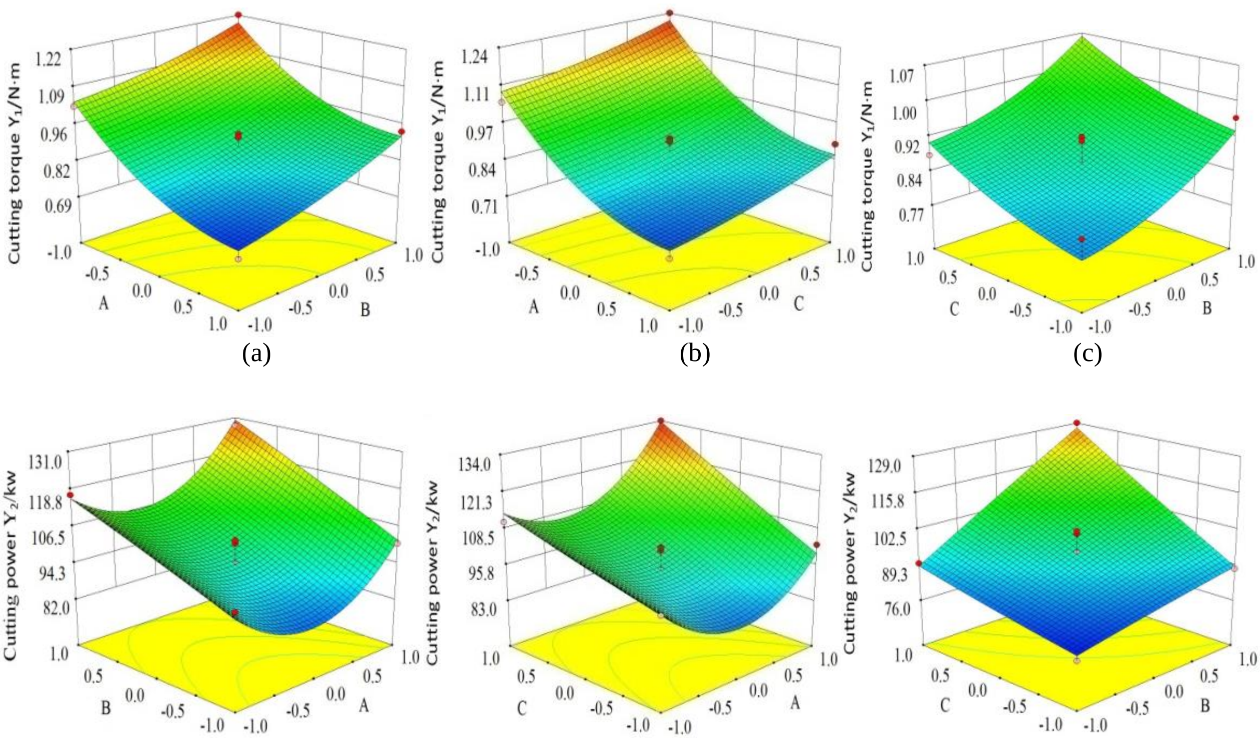

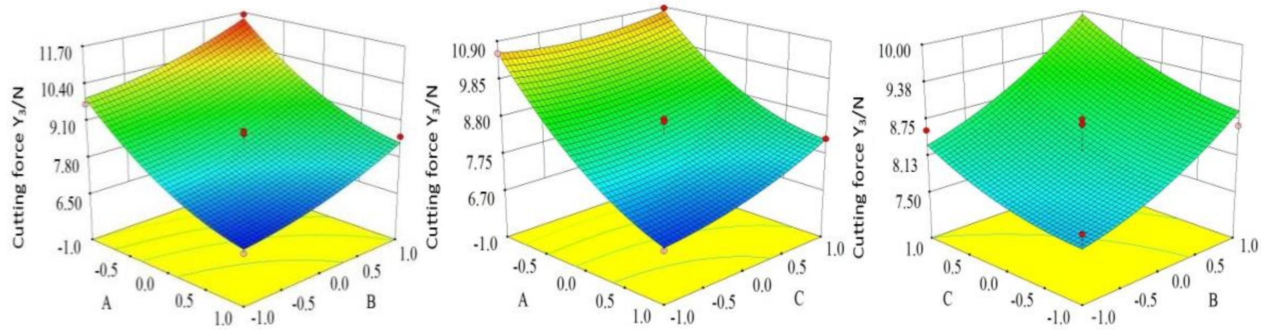

(g) (h) (i)

Fig. 6: Response surfaces influenced by interactive factors on the test index (a) Interaction between A and B, C = 1.5 kg (b) Interaction between A and C, B = 0.7 m·s-1 (c) Interaction between B and C, A = 1100 r/min; (d) Interaction between A and B, C = 1. 5 kg (e) Interaction between A and C, B = 0.7 m·s-1 (f) Interaction between B and C, A = 1100 r/min; (g) Interaction between A and B, C = 1.5 kg (h) Interaction between A and C, B = 0.7 m·s-1 (i) Interaction between B and C, A = 1100 r/min

Table 1: Test factors and levels

Levels	Factors Cutter roller speed A($r \cdot min^{-1}$)	Conveying speed B($m \cdot s^{-1}$)	Feeding amount C(kg)
-1	900	0.5	1.0
0	1100	0.7	1.5
1	1300	0.9	2.0

Table 2: Test plan and results

No.	Factors Cutter roller speed A($r \cdot min^{-1}$)	Conveying speed B($m \cdot s^{-1}$)	Feeding amount C(kg)	Index Cutting torque Y_1(N·m)	Cutting powe r Y_2(w)	Cutting force Y_3(N)
1	-1	-1	0	1.51	157	12.58
2	1	-1	0	1.10	161	9.16
3	-1	1	0	1.65	177	13.75
4	1	1	0	1.19	188	9.91
5	-1	0	-1	1.52	158	12.67
6	1	0	-1	0.83	163	6.92
7	-1	0	1	1.64	171	13.67
8	1	0	1	1.25	202	10.42
9	0	-1	-1	1.05	136	8.75
10	0	1	-1	1.23	148	10.25
11	0	-1	1	1.22	150	10.16
12	0	1	1	1.37	189	11.42
13	0	0	0	1.28	154	10.67
14	0	0	0	1.25	149	10.42
15	0	0	0	1.27	161	10.58
16	0	0	0	1.24	152	10.33
17	0	0	0	1.13	162	9.41

Table 3: Variance analysis of regression model

Index	Source	Sum of squares	Degree of freedom	Mean square	*F* value	*P* value	Significant
Cutting torque	Model	0.69	9	0.076	19.100	0.0004	**
	A	0.48	1	0.48	119.280	<0.0001	**
	B	0.039	1	0.039	9.840	0.0165	*
	C	0.090	1	0.090	22.660	0.0021	**
	AB	6.250E-004	1	6.250E-004	0.160	0.7039	
	AC	0.022	1	0.022	5.650	0.0492	*
	BC	2.250E-004	1	2.250E-004	0.056	0.8190	
	A^2	0.051	1	0.051	12.900	0.0088	**
	B^2	1.364E-003	1	1.364E-003	0.340	0.5768	

Table 3: Continue

	C^2	5.012E-003	1	5.012E-003	1.260	0.2991	
	Residual	0.028	7	3.985E-003			
	Lack of Fit	0.013	3	4.458E-003	1.230	0.4088	
	Pure Error	0.015	4	3.630E-003			
	Cor Total	0.71	16				
Cutting power	Model	4482.67	9	498.07	18.600	0.0004	**
	A	325.13	1	325.13	12.140	0.0102	*
	B	1200.50	1	1200.50	44.830	0.0003	**
	C	1431.13	1	1431.13	53.440	0.0002	**
	AB	12.25	1	12.25	0.460	0.5205	
	AC	169.00	1	169.00	6.310	0.0403	*
	BC	182.25	1	182.25	6.810	0.0350	*
	A^2	1139.38	1	1139.38	42.550	0.0003	**
	B^2	7.12	1	7.12	0.270	0.6221	
	C^2	8.85	1	8.85	0.330	0.5833	
	Residual	187.45	7	26.78			
	Lack of Fit	58.25	3	19.42	0.600	0.6477	
	Pure Error	129.20	4	32.30			
	Cor Total	4670.12	16				
Cutting force	Model	47.62	9	5.29	19.010	0.0004	**
	A	33.05	1	33.05	118.720	<0.0001	**
	B	2.74	1	2.74	9.840	0.0165	*
	C	6.27	1	6.27	22.510	0.0021	**
	AB	0.044	1	0.044	0.160	0.7025	
	AC	1.56	1	1.56	5.610	0.0497	*
	BC	0.014	1	0.014	0.052	0.8266	
	A^2	3.58	1	3.58	12.840	0.0089	**
	B^2	0.090	1	0.090	0.320	0.5866	
	C^2	0.34	1	0.34	1.220	0.3067	
	Residual	1.95	7	0.28			
	Lack of Fit	0.93	3	0.31	1.210	0.4135	
	Pure Error	1.02	4	0.26			
	Cor Total	49.57	16				

Table 4: Results of verifying tests

Cutting torque Y_1(N·m)			Cutting powerY_2(w)			Cutting forceY_3(N)		
Predicted value	Measured value	Relative error(%)	Predicted value	Measured value	Relative error(%)	Predicted value	Measured value	Relative error(%)
0.86	0.84	2.32	148.5	145.6	1.95	7.19	7.04	2.08
0.86	0.82	4.65	148.5	153.1	3.10	7.19	7.41	3.06
0.86	0.83	3.49	148.5	142.6	3.97	7.19	7.51	4.45
0.86	0.89	3.49	148.5	143.2	3.57	7.19	6.98	2.92
0.86	0.87	1.16	148.5	146.7	1.21	7.19	6.92	3.76
Average value	0.85	3.02	Average value	146.2	2.76	Average value	7.17	3.25

Model Optimization and Experimental Verification

According to the performance requirements and actual working conditions of the sweet potato vine cutting test bench, the cutting torque and cutting power must be required to be small and the cutting force must be required to be low. Due to the influence of each factor on target values being inconsistent, so a global multi-objective optimization is needed (Zhang *et al*., 2013). Taking the cutting torque Y_1, cutting power Y_2, and cutting force Y_3 as objective functions and taking the cutter roller speed x_1, conveying speed x_2, and feeding amount x_3 as design variables, the constraints of the optimized mathematical model are as follows:

$$\begin{cases} \min Y_1 = f_1(x_1, x_2, x_3) \\ \min Y_2 = f_2(x_1, x_2, x_3) \\ \min Y_3 = f_3(x_1, x_2, x_3) \\ s.t. \begin{cases} x_1 \in (900, 1300) \\ x_2 \in (0.4, 0.8) \\ x_3 \in (1, 2) \end{cases} \end{cases} \tag{22}$$

To find the optimal combination of parameters and comprehensively consider the influence of three factors on the cutting torque, cutting power, and cutting force. The parameter optimization method adopted the main objective function method and the design-Expert 8.0 software was used to optimize the solution. When the cutter roller speed is 1266.00 $r \cdot min^{-1}$, the conveying speed is 0.54 $m \cdot s^{-1}$ and the feeding amount is 1.0 kg, the cutting torque is 0.86 N·m, the cutting power is 148.5 w and the cutting force is 7.19 N.

To verify the accuracy of the regression model of cutting torque, cutting power, and cutting force, Five tests were carried out under the optimal working parameter combination.

It can be seen from Table 4, that there is a good fit between the measured value and the optimized value, the error between the measured value and the optimized value is less than 5% and the parameter optimization model is reliable and effective. Under the optimum test conditions, the cutting torque is 0.85 N·m, the cutting power is 146.2 W and the cutting force is 7.17 N.

Discussion

In this test, only the influence of the cutter roller speed, conveying speed and feeding amount on the target value was considered. The parameters such as the moisture content of sweet potato vine and the structural parameters of the cutter were not fully tested, so it is necessary to comprehensively consider the above factors in the follow-up study. At the same time, Shinshu 19 was used as the research object to study the cutting mechanism, but there are some differences between different varieties. Due to the influence of time, the cutting mechanism of sweet potato vines of other varieties cannot be systematically studied. In future research, it is necessary to improve and supplement relevant data to fully reveal the cutting mechanism of sweet potato vines. In addition, this study was mainly carried out in the laboratory using a self-made sweet potato vine cutting test bench and the test results were not applied to actual field operations. Therefore, the next step is to carry out the actual sweet potato vine cutting test in the field based on indoor research. Considering the vibration excitation of the machine caused by the ground conditions, the effect of working parameters on the cutting mechanism of sweet potato vine needs to be further studied, to provide technical support for the development of efficient and low-consumption cutter and sweet potato vine harvesting machinery.

Conclusion

A performance test platform for sweet potato vine cutting is designed in this study. Through the sweet potato vine cutting test, it is verified that the platform has the characteristics of stable operation, high measurement accuracy, and simple operation. It realizes the real-time detection of torque, power, and rotation speed. The platform can provide a reliable scientific basis for cutter design and power selection of sweet potato vine harvesting machinery.

A quadratic regression model was established with the cutting torque, cutting power, and the cutting force as response indexes by using the Box-Behnken experimental design method. Through the analysis of model interaction and response surface, the change law of the influence of the cutter roller speed, the conveying speed, and the feeding amount on the response indexes was obtained. The cutting torque and cutting force decrease with the increase of the cutter roller speed and increase with the increase of the conveying speed and feeding amount. The cutting power decreases first and then increases with the increase of the cutter roller speed and increases with the increase of the conveying speed and feeding amount.

The designed model was optimized by Design-Expert software and the accuracy of the optimization results was verified by experiments. The relative error between the measured value and the optimized value was less than 5%, indicating that the model was high reliability. When the cutter roller speed is 1266.00 r·min-1, the conveying speed is 0.54 m·s-1 and the feeding amount is 1.0kg, the cutting torque is 0.85 N·m, the cutting power is 146.2 w and the cutting force is 7.17 N. At this time, the sweet potato vine cutter has excellent working performance such as good processing stability and low energy consumption. The research results provide a reference for further improving the design of sweet potato vine harvesting machinery.

Acknowledgment

This study was supported by the General Project of Shandong Natural Science Foundation (ZR2021ME173), and the Youth Science and Technology Innovation Fund of Shandong Agricultural University (72196).

Author Contributions

Guizhi Mu and Zhengduo Liu: Performed the experiments and analyzed the data.

Wenxiu Zheng and Zhaoqin Lü: Designed and performed the experiments and prepared the paper.

Junming Liu, Xieteng Qi, and Xu Wang: Performed the experiments and revised the manuscript.

Ethics

This article is original and contains unpublished material. The corresponding author confirms that all of the other authors have read and approved the manuscript and that no ethical issues are involved.

References

Bovell-Benjamin, A. C. (2007). Sweet potato: A review of its past, present, and future role in human nutrition. Advances in food and nutrition research, 52, 1-59. doi.org/10.1016/S1043-4526(06)52001-7

Chen, X. D. (2020). Study sweet-potato-stalk separation characteristics and structure optimization of self-propelled sweet potato combine harvester. Anhui Agricultural University, Anhui, China. doi.org/10.26919/d.cnki.gannu.2020.000008

Deng, L. L., Li, Y. M., Xu, L. Z., Qing, T. D., & Pang, J. (2013). The Design and Analysis of Cutting Process about the Disc Type Corn Stalk Cutting Test Bed. Journal of Agricultural Mechanization Research. 35(01), 73-77. doi.org/10.13427/j.cnki.njyi.2013.01.046

Du, Z. (2020). Research on the biomimetic design of cutting blade for tea stem and its cutting performance. Jiangsu University, Jiangsu, China. doi.org/10.27170/d.cnki.gjsuu.2020.000113

Gibson, R. (2013). How sweet potato varieties are distributed in Uganda: Actors, constraints, and opportunities. Food Security, 5(6), 781-791. https://link.springer.com/article/10.1007/s12571-013-0302-8

Hu, L., Wang, G., Ling, X., Wang, B., Wang, B., & You, Z. (2015). Mechanical properties of sweet potato vine and stalk during harvest. Transactions of the Chinese Society of Agricultural Engineering, 31(9), 45-49. https://www.ingentaconnect.com/content/tcsae/tcsae/2015/00000031/00000009/art00008

Kakahy, A. N. N., Ahmad, D., Akhir, M. D., Sulaiman, S., & Ishak, A. (2014). Effects of Knife Shapes and Cutting Speeds of a Mower on the Power Consumption for Pulverizing Sweet Potato Vine. Key Engineering Materials. 594-595, 1126-1130. doi.org/10.4028/www.scientific.net/KEM.594-595.1126

Kakahy, A. N., Ahmad, D., Akhir, M. D., Sulaiman, S., & Ishak, A. (2014). Effects of rotary mower blade cutting angles on the pulverization of sweet potato vine. Agriculture and Agricultural Science Procedia, 2, 95-101. https://www.sciencedirect.com/science/article/pii/S2210784314000151

Liu, W. F., Chen, L. Q., Zhang, J. M. (2015). Development of test-bed for straw crushers. Journal of Machine Design. 32(02), 32-36. doi.org/10.13841/j.cnki.jxsj.2015.02.007

Lu, H. X., Tang, D. B., Wu, Z. D., Luo, K., Han, X., Jing, F., Luo, Y. L., Zhang, X. Y., Zhang, K., Wang, J. C. (2015). Genotypic variation and environmental effects on yield, quality, and agronomic traits of sweet potato. Chinese Journal of Eco-Agriculture. 23(9), 1158-1168. doi.org/10.13930/j.cnki.cjea.150363

Luthuli, C. F., Fon, F. N., & Gunya, B. (2019). Knowledge and perception of small holding farmers on supplementation and feeding sweet potato vines to goats. Pastoralism, 9(1), 1-6.

Pedrosa, C. E. andrade, V. C., Pereira, R. C., Dornas, M. F., Azevedo, A. M., & Ferreira, M. A. (2015). Yield and quality of wilted sweet potato vines and their silages. Horticultura Brasileira. 33(3), 283-289. doi.org/10.1590/S0102-053620150000300002

Pereira, R. C., Dornas, M. F. S., Ribeiro, K. G., de Souza, I. A., Agarussi, M. C. N., da Silva, V. P., ... & Pereira, O. G. (2021). Nutritive value, fermentation profile, and effluent loss in sweet potato vine silage, with or without microbial inoculant. Grassland Science, 67(1), 41-47. https://onlinelibrary.wiley.com/doi/abs/10.1111/grs.12284

Phesatcha, K., & Wanapat, M. (2013). Performance of lactating dairy cows fed a diet based on treated rice straw and supplemented with pelleted sweet potato vines. Tropical animal health and production, 45(2), 533-538. https://link.springer.com/article/10.1007/s11250-012-0255-5

Smith, S. L., & Wright, M. E. (1994). A Preharvest vine disposal machine for sweet potatoes. Applied Engineering in Agriculture, 10(3), 321-326 https://elibrary.asabe.org/abstract.asp?aid=25858.

Wang, F., Fu, Y. B., Yang, Z., Liu, P. W., Jia, Z. Y., Gao, Z. H., & Zhang, Y. (2022). Energy consumption of sunflower stalk cutting by pendulum cutting experiment. Journal of Agricultural Mechanization Research. 44 (06), 194-198. doi.org/10.13427/j.cnki.njyi.2022.06.033

Xu, S., Tong, J., & Li, M. (2017). Performance testing of vegetable chopping machine based on LabVIEW and operation parameter optimization. Transactions of the Chinese Society of Agricultural Engineering, 33(3), 250-256. https://www.ingentaconnect.com/content/tcsae/tcsae/2017/00000033/00000003/art00034

Xue, Z., Zhang, L. F., Song, G., Wang, M. W., Han, Y. F., & Wang, G. (2019). Experimental Research of Cassava Stem Cutting Based on Disc Cutter. Journal of Agricultural Mechanization Research. 41(06), 191-195-200. doi.org/10.13427/j.cnki.njyi.2019.06.035

Yuan, B., Xue, L. W., Zhang, Q. Y., Kong, W. W., Peng, J., Kou, M., & Jiang, J. H. (2016). Essential oil from sweet potato vines, a potential new natural preservative and an anti-oxidant on sweet potato tubers: Assessment of the activity and the constitution. Journal of agricultural and food chemistry, 64(40), 7481-7491. https://pubs.acs.org/doi/abs/10.1021/acs.jafc.6b03175

Zhang, S., Song, Z., Yan, Y., Li, Y., & Li, F. (2013). Development and experiment of measure and control system for stalk cutting test bench. Transactions of the Chinese Society of Agricultural Engineering, 29(25), 10-17. https://www.ingentaconnect.com/content/tcsae/tcsae/2013/00000029/00000025/art00002